

**Experimental investigation of friction performance of automotive brake using
Alumina and Titanium alloy**¹Brijendra Gupta, ²Shivam Nandev, ³Saurabh Koshti ⁴Vijay Sahu, ⁵Sumit Katare,¹Assistant Professor, Mechanical Engg. Department, Adina institute of science & technology Sagar (M.P.)
^{2,3,4,5}B.E. Research Scholar, Adina institute of science & technology Sagar (M.P.)

ABSTRACT- Brake lining materials generally are asbestos metals and ceramics. Asbestos release the hazardous gases during application which causes damage to the health. In this study had undertaken Experimental investigation of Friction performance of automotive brake using different materials namely Alumina and Titanium alloy compare with grey cast iron (GCI). In current study the wear, temperature rise and disk stopping time were investigated based on analysis better suitable material for brake lining will be selected. The test rig was used to determine the performance of the brake pads produced with the optimum manufacturing parameters and optimum composition. The pads were tested for wear, disk stopping time and temperature rise. The developed pad A (Pad of cast iron with titanium and alumina alloy) had greater wear resistance than the pad B (grey cast iron) at all speeds and loads. The comparisons for disk temperature rise and stopping time shows that the developed brake pad has about the same performance as the commercial (grey cast iron pad). The above results show that judging by the quality indices selected i.e. wear rate, average stopping time and average temperature pad A is of a greater quality than pad B. Thus it can be applied in cases where less weight is specifically required for good performance, such as Formula-1 racing cars.

KEYWORDS: - Automotive brake frictional material; Brake pad; Wear rate; Stopping time; Temperature rise.

I. INTRODUCTION

Automotive brake systems have been refined for over 100 years and have become extremely dependable and efficient. It allows the driver to slow or stop the vehicle and prevents a stationary vehicle from moving. The brake system constitutes an integral part of an automobile. A vehicle brake is a brake used to slow down a vehicle by converting its kinetic energy into heat. Failure of the automobile brake system may lead to accidents, property damage, physical injuries or death of an individual.

The major components of brake system are callipers, drum brakes, master cylinder, and hydraulic boost units, rotors, brake pedal, cables pipes, hoses, sensors and electronic systems controlling the operation of brakes. Brake lining materials generally are asbestos, metals, non - asbestos organic (NAO) such as palm kernel shell (PKS). The main element is used for brake lining from palm

Kernel shell (PKS) which is agro - waste. The average disk temperature and average stopping time for pass is increased and it has poor dimensional stability. Hence it has lost favour and several alternative materials are being replaced these days.

A potential area for new aluminium metal matrix composite (Al-MMC) applications is brake disks and drums. In general, automotive brake disks and drums are today made of cast iron or steel. Except for its relatively low wear resistance, aluminium would be a preferred material for these applications. Aluminium alloys are relatively strong and offer excellent fracture toughness.

LITERATURE REVIEW

A. O. A. Ibbhadode et al. [1] presented paper on a non – asbestos friction material was developed using an agro – waste material base - palm kernel shell (PKS) along with other constituents. Taguchi optimization technique was used to achieve optimal friction material formulation and manufacturing parameters. The derived friction material was used to produce automobile disk brake pads. The laboratory brake pads were tested for wear and effectiveness on a car. When compared with a premium asbestos-based commercial brake pad they were found to have performed satisfactorily. However, more pad wear was observed on the PKS pad at high vehicular speeds beyond 80 km/hr.

The mechanical and physical properties compare well with commercial asbestos-based friction lining material. Its performance under static and dynamic conditions compare well with the asbestos-based lining material. The results suggest that palm kernel shell could be a possible replacement for asbestos in friction lining materials.

Mustafa Boz et al. [2] give in the first stage, bronze-based brake linings were produced and friction-wear properties of them were investigated. In the second stage, 0.5%, 1%, 2% and 4% alumina (Al₂O₃) powders were added to the bronze-based powders and Al₂O₃ reinforced bronze-based brake linings were produced.

The highest friction coefficient was obtained in the samples containing Al₂O₃ in the range of 4% due to an increase in the temperature during friction. The addition of 2% Al₂O₃ to the samples showed stable friction coefficient.

K.Deepika et al. [3] enlightened about a non-asbestos bio-friction material which was developed using an Agro-waste material palm kernel shell (PKS) along with other Ingredients. Among the agro-waste shells investigated the PKS exhibited more favourable properties. Taguchi optimization technique was used to achieve optimal formulation of the friction material.

P. Filip et al. [4] concentrate on (i) the friction and wear characteristics of a newly formulated brake lining material and (ii) the impact of potassium titanate on its performance. Two different material samples were formulated, tested and analysed. The friction and wear characteristics of the first (without potassium titanate) and second (with potassium titanate) sample types were determined using the Friction Assessment and Screening Test (FAST) and a full-scale single-ended inertial type disc brake automotive dynamometer test.

The experimental results show that the friction layer, with the presence of potassium titanate, significantly improved the overall performance. Simultaneous fade reduction, stabilized friction coefficient, and wear improvements were achieved by adding potassium titanate and its contribution to the friction layer formulation.

Peter J. Blau et al. [5] inform about titanium alloys and their composites have the potential to reduce truck disc brake component weight and improve their resistance to road-salt corrosion. A titanium alloy rotor can weigh approximately 37% less than a conventional cast iron rotor with the same dimensions, while offering good high-temperature strength and much better resistance to corrosion.. Friction coefficients and temperature rise data were obtained for two commercial Ti alloys, four experimental Ti-based hard particle composites, and a thermally spray-coated Ti alloy. Several commercially produced lining materials were used as counter faces. The wear rates of the Ti metal matrix composites exceeded that of the reference cast iron, but were significantly better that of two Ti alloys. A thermal conversion parameter was used to compare the efficiency by which various material combinations convert frictional work into temperature rise. Several of the tested material combinations provided friction coefficients within the typical range for brake materials (0.35–0.55) and some showed excellent resistance to fade, a phenomenon in which braking effectiveness decreases as temperature rises. The thermally spray-coated Ti disc exhibited the least wear and merits further attention as a lightweight, corrosion-resistant brake rotor material.

II. FRICTIONAL MATERIALS

A. Asbestos

Asbestos become the major material for friction material composition over eight decade and become more wide spread during the industrial revolution in 1866. Asbestos were from Greek word which mean "unquenchable" or "inextinguishable" is a set of six naturally occurring silicate minerals exploited commercially for their desirable physical properties.

B. Kevlar or Aramid

The use of non-metallic friction material seems to become the solution forth asbestos friction material. Friction material made from Kevlar or aramid fiber.

Aramid fiber a generic expression denoting fiber made from the condensation product of isophthalic orterephthalic acids and morphenylene diamine such as Kelvar fibre sareal so widely used as reinforcing fiber ,but they are a deferent class of fiber in that the relatively so fiber. They are very light an excellent thermal stability, with a very good stiffness to weight ratio.

C. Fibertuff

Fibertuff is a product designed to give the wear of a ceramic facing, yet have the engagement and disengagement qualities of an organic material. Fibertuff intended to wear against its mating surfaces like organic material. Used primarily in the stamped steel and cast units, this product offers greater life than organic material with many of the same qualities that organic friction has traditionally offered. Around-town delivery trucks and mid-range applications find that this product works best.

D. Non – asbestos friction materials

It was developed using an agro – waste material base - palm kernel shell (PKS) along with other constituents. Taguchi optimization technique was used to achieve optimal friction material formulation and manufacturing parameters. The mechanical and physical properties compare well with commercial asbestos-based friction lining material. Its performance under static and dynamic conditions compare well with the asbestos-based lining material. From both results suggest that palm kernel shell could be a possible replacement for asbestos in friction lining materials. We can improve the properties further by changing the composition of a brake pad material (PKS).

E. Bronze-based powders and Al₂O₃ reinforced brake linings materials

The highest friction coefficient was obtained in the samples containing Al₂O₃ in the range of 4% due to an increase in the temperature during friction. The addition of 2% Al₂O₃ to the samples showed stable friction coefficient.

F. Friction layer with the presence of potassium titanate

The Friction Assessment and Screening Test (FAST) and a full-scale single-ended inertial type disc brake automotive dynamometer test results show that the friction layer, with the presence of potassium titanate, significantly improved the overall performance.

G. Iron oxide and graphite materials

Solid lubricants like graphite affected the friction and wear behaviour of Fe₃O₄ powders considerably whereas further addition of hard nanoparticles induced only minor effects. The latter could be explained, after nanoscopic characterization, by oxidation and destruction of the wear-protecting tribofilm.

H. Titanium alloys

A titanium alloy rotor can weigh approximately 37% less than a conventional cast iron rotor with the same dimensions, while offering good high-temperature strength and much better resistance to corrosion. The thermally spray-coated Ti disc exhibited the least wear and merits further attention as a lightweight, corrosion-resistant brake rotor material. It has high hardness properties (300BHN).

I. Cryogenic processing of grey cast iron

Cryogenic treatment affects the whole cross-section of the component and is inexpensive compared to other treatment processes.

The results indicate an improvement in the wear rate of grey cast iron of 9.1–81.4% due to deep cryogenic treatment where significant wear has occurred, although there was no significant change in the bulk hardness, matrix hardness or in the microstructure of the material under optical observation.

J. Semi metallic friction materials

Its functionality a wear test was conducted on a commercial brake pad at various pressure speeds and inertia load. This prototype test rig can be used in testing the brake pad of different vehicle such as Maruti, Tata, Nissan, Toyota, Mitsubishi, Volvo, Peugeot, and other brands of interest. With little modification, this product can be commercialized.

III. EXPERIMENTAL SETUP

A. Test rig

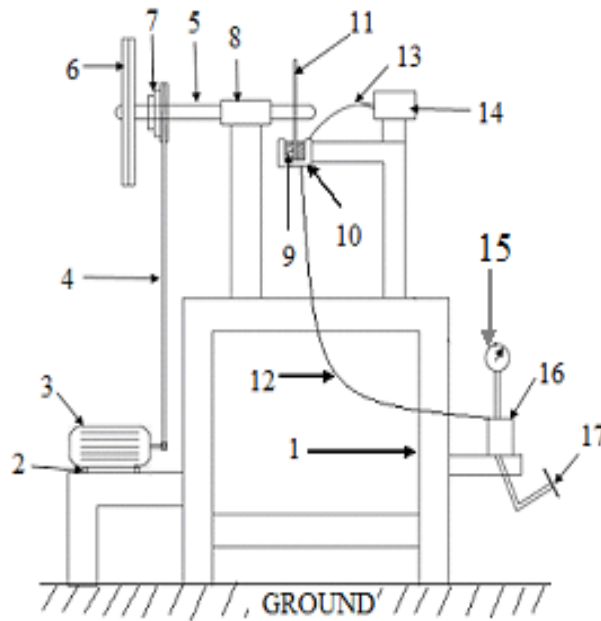
The test rig was used to determine the performance of the brake pads produced with the optimum manufacturing parameters and optimum composition. The pads were tested for wear, disk stopping time and temperature rise.

Fig.1 shows the schematic diagram of the brake pad test rig. It has a 1.5 kW (2 hp, 1100 rpm) motor with a provision for speed variation by using a stepped pulley. The motor provides the energy required to set the flywheel weights and the brake disc in angular motion. When a set of brake pad is fixed into the brake caliper assembly of the test rig, the system is switch-on and the drive shaft begins to rotate, it is then allowed to attain a desired speed. Thereafter, a manual force is applied on the brake pedal which is similar to that of a motor car. Subsequently the stopping time and temperature brake pad material lost are easily obtained. The rig also incorporates a hydraulic circuit fitted with a pressure gauge to measure the pressure in the fluid line from which the force with which the brake pad push against the disc can be estimated. The speed and brake line pressure ranges were: 685 to 950 rpm and 8 to 14 bar respectively for the test conditions.

B. Performance tests

A performance test was carried out on the constructed rig to determine its functionality by investigating the effect of speed and contact pressure on wear of a brake pad material. The test was carried out on two sets of brake pads from different MMC and cast iron is labelled pads A and B respectively. The test was carried out in two phases first Keeping contact pressure constant and varying rotating speed of the brake disc (ranging from 685 to 950 rpm), keeping rotating speed constant and varying contact pressure (ranging from 8 to 14bar).

The wear rates, average stopping time and average temperature of both sets of brake pads (PAD A-With titanium and alumina alloy, PAD B-Grey cast iron) being tested under the above conditions were measured and recorded.



- | | |
|--------------------|----------------------------|
| 1. Frame | 10. Brake caliper assembly |
| 2. Parking pad | 11. Brake disc |
| 3. Electric motor | 12. Brake Pipe |
| 4. V Belt | 13. J Type Thermocouple |
| 5. Shaft | 14. Temperature Indicator |
| 6. Fly wheel | 15. Pressure gauge |
| 7. Step Pulley | 16. Brake fluid reservoir |
| 8. Bearing housing | 17. Brake pedal |
| 9. Brake Pad | |

Fig.1: Schematic representation of the brake pad test rig

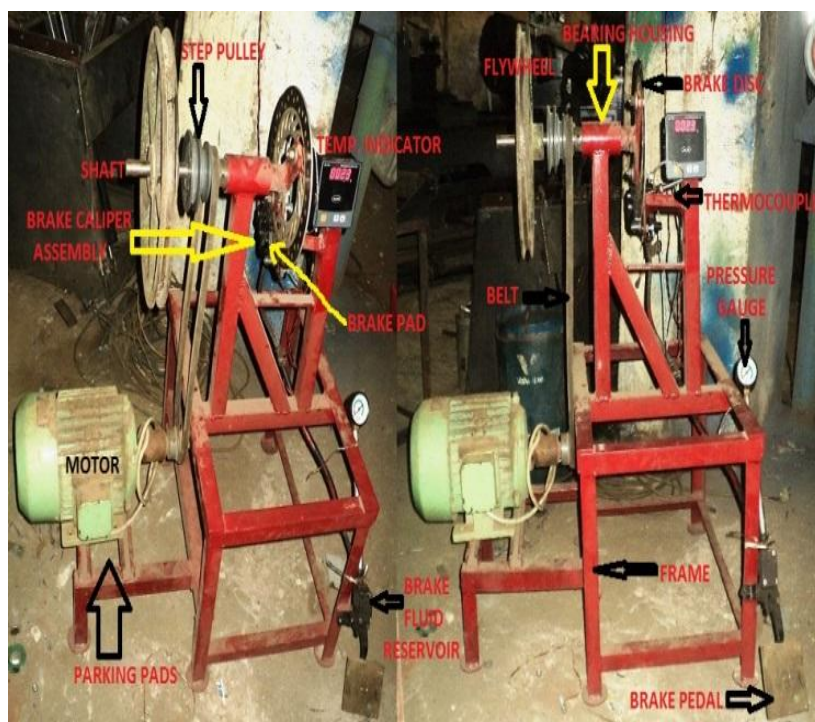


Fig. 2: Brake pad test rig

Table 1: Components specification of brake pad test rig

S.N.	COMPONENT	SPECIFICATION
1	Frame	Material = Cast iron Vertical length = 0.8= 800mm E of iron = 100 GPa Size = 30×30×3mm square channel And 30×30×2mm angle iron Joint = MSG12 electrode welding
2	Motor	Speed = 1100rpm Power = 1.5kw = 2HP Motor sheave dia.=56mm
3	Step pulley	Dimensions = 90, 70, 65mm dia.
4	V Belt	Thickness = 10 mm Length = 1.2m = 1200mm
5	Centre distance belt to pulley	C = 0.35m = 350mm
6	Bearing	2-20mm ball grove with external dia.42mm 2-20mm cylindrical roller with external dia.42mm
7	Bearing housing	200×150×4mm plate Fold in cylindrical shape = 150×50mm dia.
8	Main drive shaft	35 mm to 20 mm in Centre, lathe
9	Brake disc	Radius = 11 cm = 110 mm Thickness = 10 mm Mass = 3.54 Kg
10	Brake pad	Radius = 20mm, Thickness = 15mm, Mass = 145gram
11	Pressure gauge	0-14 bar
12	Flywheel	Mass = 7.8Kg Radius = 0.21m = 21mm Thickness = 11.3mm
13	Thermocouple J Type	Capacity 0-400 (°C)
14	Temp. Indicator	Capacity 0-400 (°C)
15	Test condition	685 - 940rpm, 8 - 12bar

IV. RESULTS AND DISCUSSION

The wear rates , average stopping time and average temperature of both sets of brake pads (PAD A-With titanium and alumina alloy, PAD B-Grey cast iron) being tested under the above conditions were measured and recorded.

PAD A – With titanium & alumina alloy brake pad.

PAD B – Grey cast iron brake pad.

Table 2: Effect of speed on brake pad wear at constant contact pressure of 8 bars

REDUCTION IN THICKNESS AFTER 50 BRAKE APPLICATIONS (mm)			WEAR PER BRAKE APPLICATION ($\times 10^{-3}$ mm)		
Speed of brake disc (rpm)	Pad A	Pad B	Speed of brake disc (rpm)	Pad A	Pad B
685	0.029	0.032	685	0.58	0.64
884	0.031	0.035	884	0.62	0.70
950	0.032	0.037	950	0.64	0.74

Table 2: Presents data on the effect of Speeds (685 rpm, 884 rpm, 950 rpm) on wear in terms of reduction in thickness for the two sets of brake pads (PAD A-With titanium and alumina alloy, PAD B-Grey cast iron). From the table, it can be deduced that the wear rate of pad A at a constant pressure of 8 bar was (0.029 mm, 0.031 mm, 0.032 mm) per 50 brake application and that of pad B was (0.032 mm, 0.035 mm, 0.037 mm) per 50 brake application on Speeds (685, 884, 950) respectively. It is evident that pad A has a shorter wear rate than pad B. A Digital micrometre was used to measure the reduction in thickness after 50 brake applications. The choice of 50 brake applications was such that an appreciable and measurable reduction in thickness could be obtained after which the average of the values were taken to reflect the reduction in thickness per brake application.

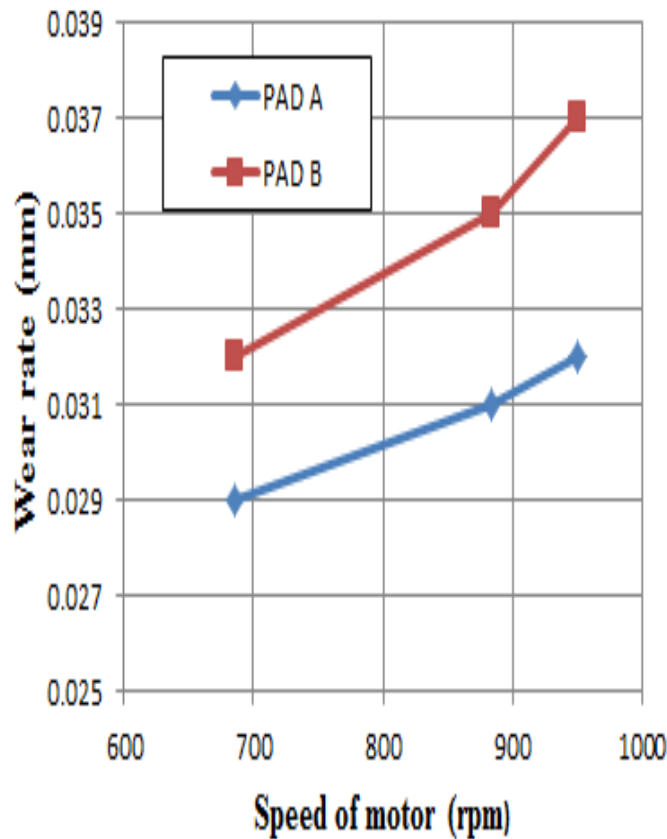


Fig.3: Graph between speed of motor and wear rate per 50 brake application at constant pressure 8 bar

Table 3: Effect of speed on brake pad wear and average stopping time (sec.) at constant contact pressure of 8 bars

Speed of brake disc (rpm)	REDUCTION IN THICKNESS AFTER 50 BRAKE APPLICATIONS (mm)		AVERAGE STOPPING TIME (Sec.)	
	Pad A	Pad B	Pad A	Pad B
685	0.029	0.032	2.92	2.98
884	0.031	0.035	3.88	4.03
950	0.032	0.037	4.25	4.49

Table 3: Presents data on the effect of Speeds (685 rpm, 884 rpm, 950 rpm) on average stopping time for the two sets of brake pads (PAD A-With titanium and alumina alloy, PAD B-Grey cast iron).From the table, it can be deduced that average stopping time of pad A at a constant pressure of 8 bar was (2.92 Second, 3.88 Second,4.25 Second) per brake application and that of pad B was (2.98 Second, 4.03 Second,4.49 Second) per brake application on Speeds (685,884,950) respectively. It is evident that pad A has a shorter stopping time than pad B. A Stop watch was used to measure the stopping time on per brake applications.

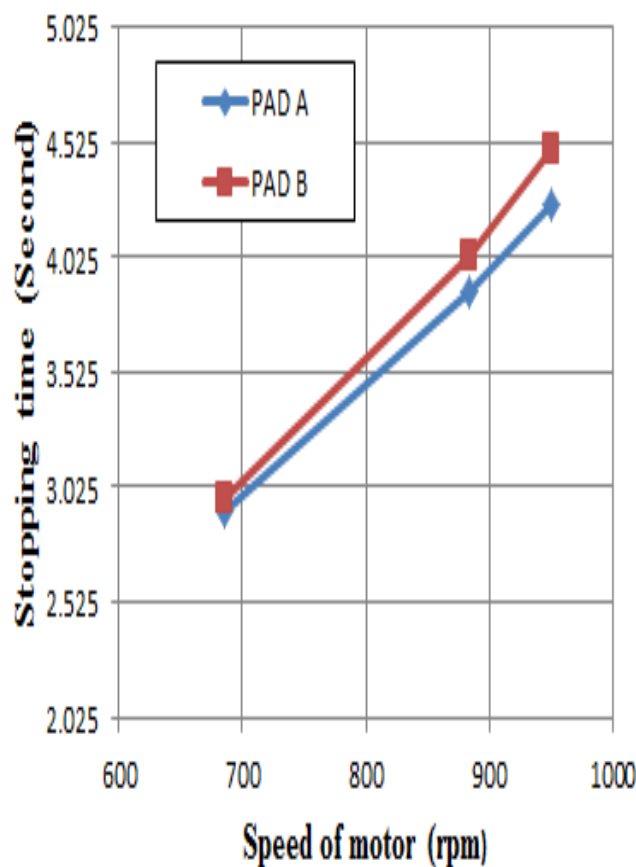


Fig.4: Graph between speed of motor and average stopping time per brake application at constant pressure 8 bar

Table 4: Effect of speed on brake pad wear and temperature ($^{\circ}\text{C}$) at constant contact pressure of 8 bars

Speed of brake disc (rpm)	REDUCTION IN THICKNESS AFTER 50 BRAKE APPLICATIONS (mm)		AVERAGE TEMPERATURE ($^{\circ}\text{C}$)	
	Pad A	Pad B	Pad A	Pad B
685	0.029	0.032	49	48
884	0.031	0.035	53	51
950	0.032	0.037	56	53

Table 4: Presents data on the effect of Speeds (685,884,950) on average temperature for the two sets of brake pads (PAD A-With titanium and alumina alloy, PAD B-Grey cast iron).From the table, it can be deduced that average temperature of pad A at a constant pressure of 8 bar was (49 $^{\circ}\text{C}$, 53 $^{\circ}\text{C}$, 56 $^{\circ}\text{C}$) per brake application and that of pad B was (48 $^{\circ}\text{C}$, 51 $^{\circ}\text{C}$, 53 $^{\circ}\text{C}$) per brake application on Speeds (685,884,950) respectively. It is evident that pad A has a higher Temperature than pad B means heat flow rate of pad A has a higher than pad B so pad A has less stopping time. A Temperature indicator was used to measure the temperature on per brake applications.

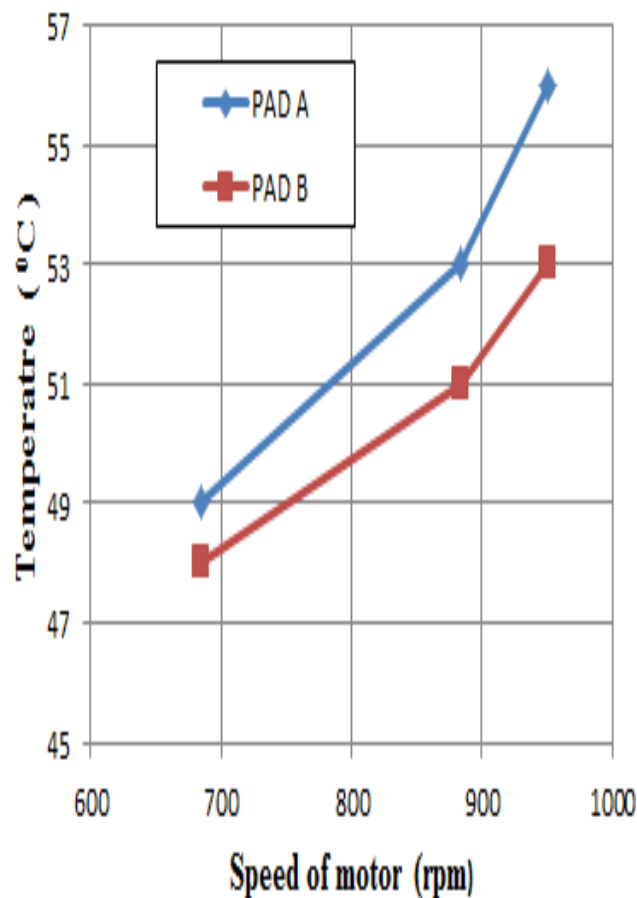


Fig.5: Graph between speed of motor and average Temperature per brake application at constant pressure 8 bar

Table 5: Effect of speed on brake pad wear at constant contact pressure of 10 bars

REDUCTION IN THICKNESS AFTER 50 BRAKE APPLICATIONS (mm)			WEAR PER BRAKE APPLICATION (X10-3 mm)		
Speed of brake disc (rpm)	Pad A	Pad B	Speed of brake disc (rpm)	Pad A	Pad B
685	0.034	0.038	685	0.68	0.76
884	0.035	0.041	884	0.70	0.82
950	0.037	0.043	950	0.74	0.86

Table 5: Presents data on the effect of Speeds (685 rpm, 884 rpm, 950 rpm) on wear in terms of reduction in thickness for the two sets of brake pads (PAD A-With titanium and alumina alloy, PAD B-Grey cast iron). From the table, it can be deduced that the wear rate of pad A at a constant pressure of 10 bar was (0.034 mm, 0.035 mm, 0.037 mm) per 50 brake application and that of pad B was (0.038 mm, 0.041 mm, 0.043 mm) per 50 brake application on Speeds (685, 884, 950) respectively. It is evident that pad A has a shorter wear rate than pad B. A Digital micrometre was used to measure the reduction in thickness after 50 brake applications. The choice of 50 brake applications was such that an appreciable and measurable reduction in thickness could be obtained after which the average of the values were taken to reflect the reduction in thickness per brake application.

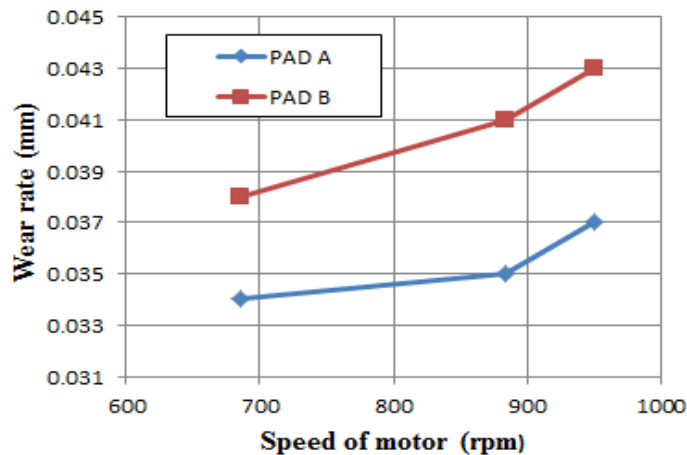


Fig.6: Graph between speed of motor and wear rate per 50 brake application at constant pressure 10 bar

Table 6: Effect of speed on brake pad wear and average stopping time (sec.) at constant contact pressure of 10 bars

Speed of brake disc (rpm)	REDUCTION IN THICKNESS AFTER 50 BRAKE APPLICATIONS (mm)		AVERAGE STOPPING TIME (Sec.)	
	Pad A	Pad B	Pad A	Pad B
685	0.034	0.038	2.69	2.74
884	0.035	0.041	3.60	3.73
950	0.037	0.043	3.90	4.17

Table 6: Presents data on the effect of Speeds (685 rpm, 884 rpm, 950 rpm) on average stopping time for the two sets of brake pads (PAD A-With titanium and alumina alloy, PAD B-Grey cast iron).From the table, it can be deduced that average stopping time of pad A at a constant pressure of 10 bar was (2.69 Second, 3.60 Second,3.90 Second) per brake application and that of pad B was (2.74 Second, 3.73 Second,4.17 Second) per brake application on Speeds (685,884,950) respectively. It is evident that pad A has a shorter stopping time than pad B. A Stop watch was used to measure the stopping time on per brake applications.

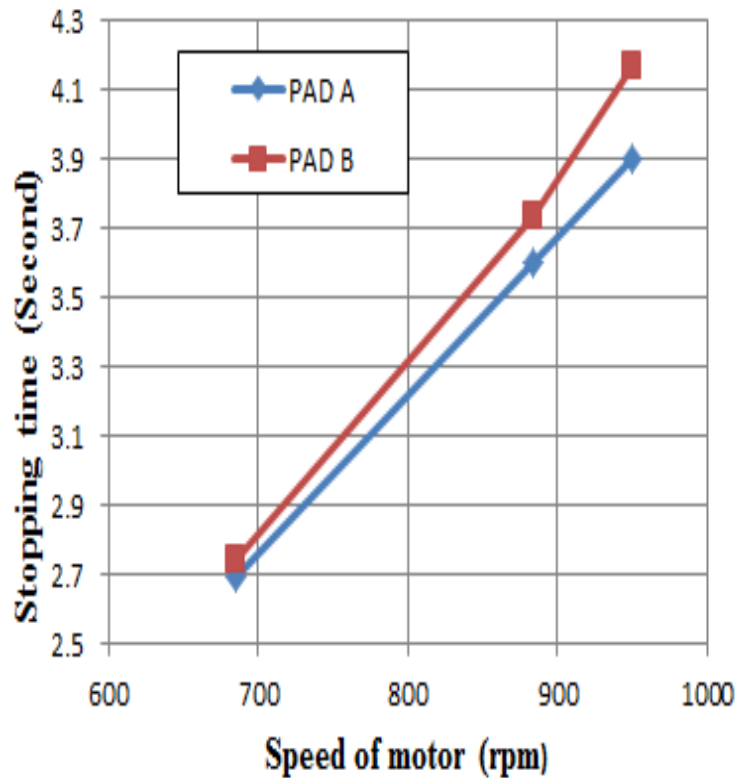


Fig.7: Graph between speed of motor and average stopping time per brake application at constant pressure 10 bar

Table 7: Effect of speed on brake pad wear and temperature (°C) at constant contact pressure of 10 bars

Speed of brake disc (rpm)	REDUCTION IN THICKNESS AFTER 50 BRAKE APPLICATIONS (mm)		AVERAGE TEMPERATURE (°C)	
	Pad A	Pad B	Pad A	Pad B
685	0.034	0.038	53	52
884	0.035	0.041	57	55
950	0.037	0.043	61	57

Table 7: Presents data on the effect of Speeds (685,884,950) on average temperature for the two sets of brake pads (PAD A-With titanium and alumina alloy, PAD B-Grey cast iron).From the table, it can be deduced that average temperature of pad A at a constant pressure of 10 bar was (53 °C, 57 °C, 61 °C) per brake application and that of pad B was (52 °C, 55 °C, 57 °C) per brake application on Speeds (685,884,950) respectively. It is evident that pad A has a higher Temperature than pad B means heat flow rate of pad A has a higher than pad B so pad A has less stopping time. A Temperature indicator was used to measure the temperature on per brake applications.

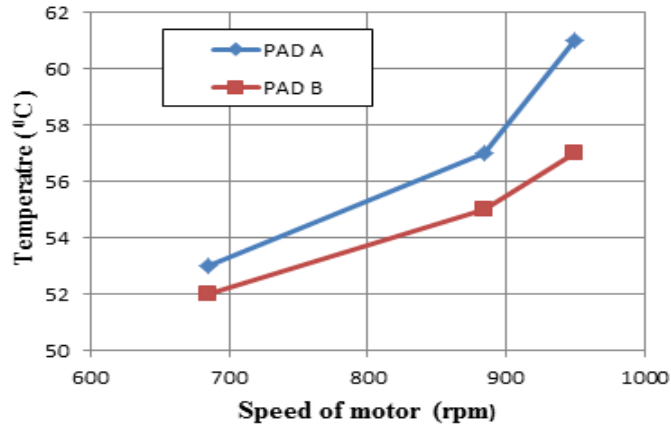


Fig.8: Graph between speed of motor and average Temperature per brake application at constant pressure 10 bar

Table 8: Effect of speed on brake pad wear at constant contact pressure of 12 bars

REDUCTION IN THICKNESS AFTER 50 BRAKE APPLICATIONS (mm)			WEAR PER BRAKE APPLICATION (X10 ⁻³ mm)		
Speed of brake disc (rpm)	Pad A	Pad B	Speed of brake disc (rpm)	Pad A	Pad B
685	0.039	0.043	685	0.78	0.86
884	0.041	0.048	884	0.82	0.96
950	0.043	0.051	950	0.86	1.02

Table 8: Presents data on the effect of Speeds (685 rpm, 884 rpm, 950 rpm) on wear in terms of reduction in thickness for the two sets of brake pads (PAD A-With titanium and alumina alloy, PAD B-Grey cast iron). From the table, it can be deduced that the wear rate of pad A at a constant pressure of 12 bar was (0.039 mm, 0.041 mm, 0.043 mm) per 50 brake application and that of pad B was (0.043 mm, 0.048 mm, 0.051 mm) per 50 brake application on Speeds (685, 884, 950) respectively. It is evident that pad A has a shorter wear rate than pad B. A Digital micrometre was used to measure the reduction in thickness after 50 brake applications. The choice of 30 brake applications was such that an appreciable and measurable reduction in thickness could be obtained after which the average of the values were taken to reflect the reduction in thickness per brake application.

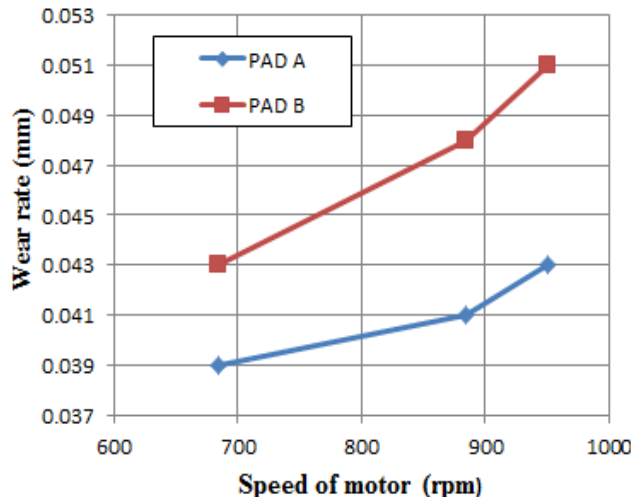


Fig.9: Graph between speed of motor and wear rate per 50 brake application at constant pressure 12 bars

Table 9: Effect of speed on brake pad wear and average stopping time (sec.) at constant contact pressure of 12 bars

Speed of brake disc (rpm)	REDUCTION IN THICKNESS AFTER 50 BRAKE APPLICATIONS (mm)		AVERAGE STOPPING TIME (Sec.)	
	Pad A	Pad B	Pad A	Pad B
685	0.039	0.043	2.50	2.54
884	0.041	0.048	3.36	3.47
950	0.043	0.051	3.71	3.89

Table 9: Presents data on the effect of Speeds (685 rpm, 884 rpm, 950 rpm) on average stopping time for the two sets of brake pads (PAD A-With titanium and alumina alloy, PAD B-Grey cast iron).From the table, it can be deduced that average stopping time of pad A at a constant pressure of 12 bar was (2.50 Second, 3.36 Second,3.71 Second) per brake application and that of pad B was (2.54 Second, 3.47 Second, 3.89 Second) per brake application on Speeds (685,884,950) respectively. It is evident that pad A has a shorter stopping time than pad B. A Stop watch was used to measure the stopping time on per brake applications.

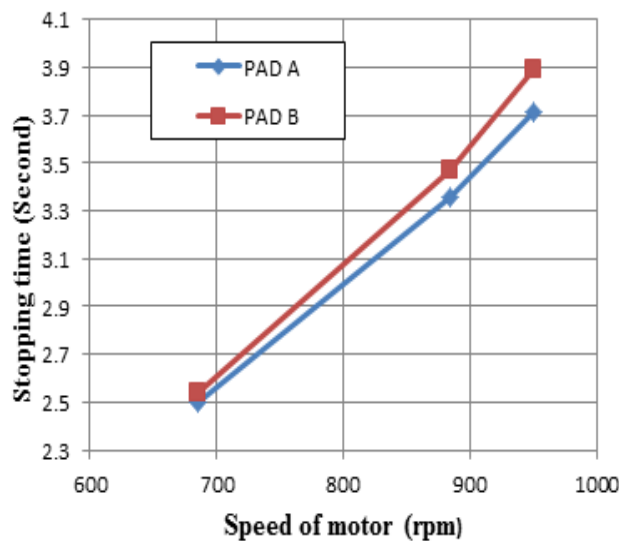


Fig.10: Graph between speed of motor and average stopping time per brake application at constant pressure 12 bar

Table 10: Effect of speed on brake pad wear and temperature (°C) at constant contact pressure of 12 bars

Speed of brake disc (rpm)	REDUCTION IN THICKNESS AFTER 50 BRAKE APPLICATIONS (mm)		AVERAGE TEMPERATURE (°C)	
	Pad A	Pad B	Pad A	Pad B
685	0.039	0.043	57	56
884	0.041	0.048	61	59
950	0.043	0.051	64	61

Table 10: Presents data on the effect of Speeds (685,884,950) on average temperature for the two sets of brake pads (PAD A-With titanium and alumina alloy, PAD B-Grey cast iron).From the table, it can be deduced that average temperature of pad A at a constant pressure of 12 bar was (57 °C, 61 °C, 64 °C) per brake application and that of pad B was (56 °C, 59 °C, 61 °C) per brake application on Speeds (685,884,950) respectively. It is evident that pad A has a higher Temperature than pad B means heat flow rate of pad A has a higher than pad B so pad A has less stopping time. A Temperature indicator was used to measure the temperature on per brake applications.

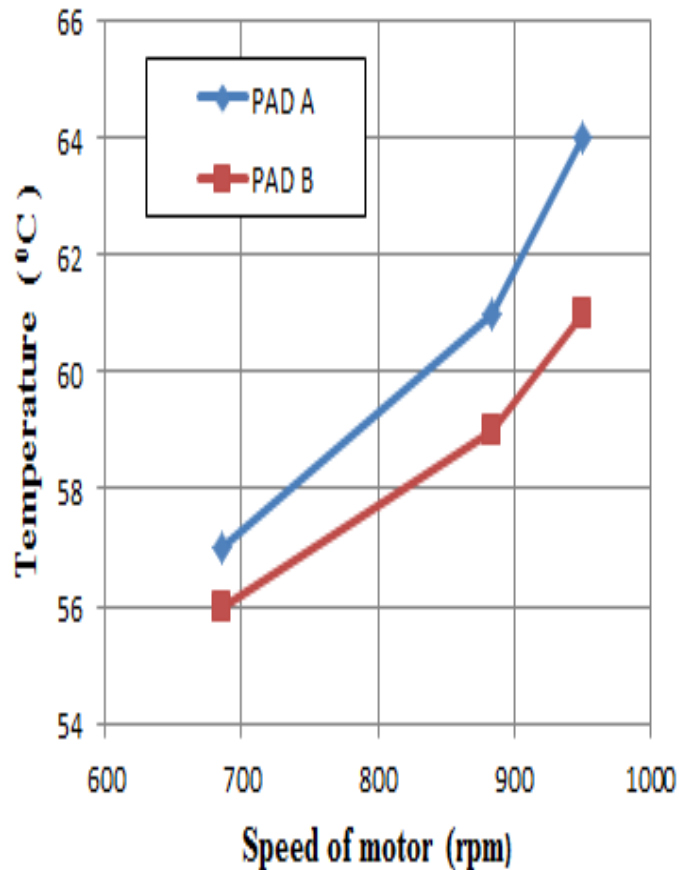


Fig.11: Graph between speed of motor and average Temperature per brake application at constant pressure 12 bar

The developed pad had greater wear resistance than the grey cast iron pad at all speeds and loads. The comparisons for disk temperature rise and stopping time shows that the developed brake pad has about the same performance as the commercial (grey cast iron pad). The above results show that judging by the quality indices selected i.e. wear rate, average stopping time and average temperature pad A (Pad of cast iron with titanium and alumina alloy) is of a greater quality than pad B(Pad of grey cast iron).

A moving vehicle possesses kinetic energy whose value depends on the weight and speed of the vehicle. In a vehicle, the engine provides this energy in order to accelerate the vehicle from standstill to a particular speed. But this energy must be dissipated when the vehicle is slowed down in the form of heat. Therefore it is the function of the brake to convert the kinetic energy possessed by the vehicle into heat energy by means of friction. As we know the kinetic energy of the vehicle would convert into heat energy when brake is applied. In order to manage with the above mentioned properties cast iron brake pad are preferred.

In the recent advancement in the development of new lightweight materials, Aluminium alloys play a significant role. It has higher thermal conductivity (247 W/mK), better wear resistance, and good corrosion resistance in addition to lightweight. Because of higher thermal conductivity Aluminium alloys dissipate heat at very faster rate. Realizing the advantages of Al alloys, it is proposed to make brake pad out of Al-Ti alloys and test their braking properties. In the recent past little research work is reported in the open literature about the investigation of Al alloy brake pads and compared with the cast iron counterpart. In the present investigation, a test rig for brake pad was used to investigate the braking parameters such as wear rate, temperature rise, stopping distance etc. Various speeds i.e., 685, 884 and 950 RPM were used for evaluation. Braking pressure of 8 to 12 bar was used in the experiments.

A. Wear rate effect:

The graphical representations shown in Fig. 3, 6 and 9 illustrate the wear behaviour of the different brake pad materials' composition. How the constituent materials affect the general performance of the brake pad materials can be understood from these figures. As can be seen from Fig. 3, 6 and 9 The reason is that as the rate of application of the braking load is increased, the rate of conduction of heat from the surface of the brake pad becomes improved by the constituent materials which the brake pad is made up of and thus the brake pad can withstand high wear out at constant application of the brake load for a long period of time. The superior wear property of the specimens is largely due to the good thermal conductivities of individual material constituents that make up the specimens. The main components that helped to improve the thermal conductivity of the brake pad are copper, aluminium and zinc. The main components that helped to improve the thermal wear resistance of the brake pad are Titanium (Hardness of titanium is 300 BHN).

B. Stopping time effect:

The graphical representations shown in Fig. 4, 7 and 10 illustrate the stopping time behaviour of the different brake pad materials' composition. How the constituent materials affect the general performance of the brake pad materials can be understood from these figures. As can be seen from Fig. 4, 7 and 10 the stopping time on the brake pads material was proportional to the applied braking load and speed. This was followed by a decrease stopping time as the duration of the braking load application is increased. The reason is that if brake load or speed increased then temperature rise increased so heat energy flow rate will be increased.

C. Temperature rise effect:

The graphical representations shown in Fig. 5, 8 and 11 illustrate the stopping time behaviour of the different brake pad materials' composition. How the constituent materials affect the general performance of the brake pad materials can be understood from these figures. As can be seen from Fig. 5, 8 and 11 the temperature rise on the brake pads material was proportional to the applied braking load. This was followed by an increase temperature rise as the braking load application is increased. The reason is that if brake load or speed increased then friction between brake pad and brake disc increased so temperature rise will be increased.

V. CONCLUSION

The Design and construction of the Experimental Brake Pad Test Rig was a successful one. The performance was satisfactory when it was used to determine the wear rate, stopping time and temperature of brake pads. The following conclusions can be made from the results discussed above. In the case of the brake pads, the alternative material - Alumina and titanium alloy with cast iron, is suitable for the required function of a friction pad material. It is an appropriate replacement for it as a friction material in brake pads.

AMC (Aluminium meal composite) has a lower density and higher thermal conductivity as compared to GCI (grey cast iron) and it results in weight reduction of up to 40% in brake systems. It is observed that higher the brake force lower is the stopping distance. The relation for speed is just reverse i.e., at higher speed the stopping distance is more. Example -

The Stopping time of cast iron with titanium and alumina alloy pad is 2.92 second, whereas in grey cast iron pad it is 2.98 second at 685 rpm and pressure 8 bar (as fig. 5.2). The Stopping time of cast iron with titanium and alumina alloy pad is 2.50 second, whereas in grey cast iron pad it is 2.54 second at 685 rpm and pressure 12 bar (as fig. 5.8). The Stopping time of cast iron with titanium and alumina alloy pad is 2.50second, whereas in grey cast iron pad it is 2.54 second at 685 rpm and pressure 12 bar (as fig. 5.8). The Stopping time of cast iron with titanium and alumina alloy pad is 3.71second, whereas in grey cast iron pad it is 3.89 second at 950 rpm and pressure 12 bar (as fig. 5.8)..

Similarly the temperature rise of cast iron with titanium and alumina alloy pad is 61 °C, whereas in grey cast iron pad it is 59 °C at 950 rpm and pressure 12 bar (as fig. 5.9). The temperature rise of cast iron with titanium and alumina alloy pad is 49 °C, whereas in grey cast iron pad it is 48 °C at 685 rpm and pressure 8 bar (as fig. 5.3). The developed pad had greater wear resistance than the grey cast iron pad at all speeds and loads. The comparisons for disk temperature rise and stopping time shows that the developed brake pad has about the same performance as the commercial (grey cast iron pad).

The above results show that judging by the quality indices selected i.e. wear rate, average stopping time and average temperature pad A (Pad of cast iron with titanium and alumina alloy) is of a greater quality than pad B (Pad of grey cast iron). Thus it can be applied in cases where less weight is specifically required for good performance, such as Formula-1 racing cars.

References

- [1] A. O. A. Ibhádodé, I. M. Dagwa, "Development of asbestos-free friction lining material from palm kernel shell", *J. Braz. Soc. Mech. Sci. & Eng.* vol.30 no.2, ISSN 1678-5878, 2008
- [2] Mustafa Boz, Adem Kurt, "The effect of Al₂O₃ on the friction performance of automotive brake friction materials", *Tribology International*, Vol. 40, Issue 7, (2007) pp. 1161-1169
- [3] K.Deepika, C.Bhaskar Reddy, "D.Ramana Reddy, Fabrication and performance evaluation of a composite material for wear resistance application", vol. 2, issue 6, ISSN 2319-5967, (2013) pp.66-71
- [4] K.W.Hee, P.Filip, "Performance of ceramic enhanced phenolic matrix brake lining materials for automotive brake linings", *wear* 259, (2005) pp.1088-1096
- [5] Peter J. Blau, Brian C. Jolly, Jun Qu, William H. Peter, Craig A. Blue, "Tribological investigation of titanium-based materials for brakes", Vol. 263, Issue 7, ISSN 0043-1648, (2007) pp. 1202-1211
- [6] W.Osterle, C.Deutsch, T.Gradt, G.Orts-Gil, T.Schneider, A.I.Dmitriev, "Tribological screening tests for the selection of raw materials for automotive brake pad formulations", *Tribology International* 73, (2014) PP.148–155
- [7] A.Akay, O.Giannini, F.Massi, A.Sestieri, "Disc brake squeal characterization through simplified test rigs", *Mechanical systems and signal processing* 23, (2009) pp. 2590–2607
- [8] R. Thornton, T. Slatter, A.H. Jones, R. Lewis, "The effects of cryogenic processing on the wear resistance of grey cast iron brake discs", *wear* 271, (2011) pp.2386-2395
- [9] P.D.Neis, N.F.Ferreira, F.P.daSilva, "Comparison between methods for measuring wear in brake friction materials". *wear* 319, (2014) pp.191-199
- [10] K.W. Liew, Umar Nirmal, "Frictional performance evaluation of newly designed brake pad materials", *material and design* 48, (2013) pp. 25-33
- [11] Bhabani K. Satapathy, Abhijit Majumdar, Harjeet S. Jaggi, Amar Patnaik, Bharat S. Tomar, "Targeted material design of flyash filled composites for friction braking application by non-linear regression optimization technique", *Computational Materials Science* 50, (2011) pp. 3145–3152
- [12] K.K. Ikpambese, D.T. Gundu, L.T. Tuleun, "Evaluation of palm kernel fibers (PKFs) for production of asbestos-free automotive brake pads", *journal of king saud university engineering science* 2014
- [13] Ashafi'e Mustafa, Mohd Fadzli Bin Abdollah, Fairuz Fazillah Shuhimi, Nurhidayah Ismail, Hilmi Amiruddin, Noritsugu Umehara, "Selection and verification of kenaf fibres as an alternative friction material using Weighted Decision Matrix method", *materials and design* 2014 pp. 1-6
- [14] Abdulwahab A. Alnaqi, David C. Barton, Peter C. Brooks, "Reduced scale thermal characterization of automotive disc brake", *applied thermal engineering* 2014 pp. 1-11
- [15] Bashar dan asabe, Peter B madakson, Joseph manji, "Material Selection and Production of a Cold-Worked Composite Brake Pad", *World J of Engineering and Pure and Applied Sci.* 92, ISSN 2449-0582, 2012
- [16] Arun Bhuneriya, Dr. Rohit Rajvaidya, P.K.Pandey, "Development of Composition of Composite Material Used For Automotive Brake Liner", vol. 2, issue 3,ISSN 2322-0821, (2014) PP. 8-13
- [17] Deepak Biradar, M. R. Chopade and S. B. Barve, "Experimental Analysis and Investigation for Thermal Behaviour of Ventilated Disc Brake Rotor using CFD", vol. 4 no. 5, ISSN 2347-5161, (2014) pp. 3339-3345
- [18] Nosa Idusuyi, Ijeoma Babajide, Oluwaseun. K. Ajayi and Temilola. T. Olugasa, "A Computational Study on the Use of an Aluminium Metal Matrix Composite and Aramid as Alternative Brake Disc and Brake Pad Material", *Hindawi Publishing Corporation Journal of Engineering Volume* 2014, Article ID 494697, (2014) pp.1-6
- [19] M. Sutikno, P. Marwoto, S. Rustad, "The mechanical properties of carbonized coconut char power-based friction materials", *carbon* 48, (2010) pp. 3616-3620
- [20] Ashish D. Dhangar, R. J. Jani, Hiren Bagada, "An Experimental Investigation of Effect of Process Parameters on Wear of Semi Metallic Automotive Disc Brake Friction Material", vol. 2, issue 3, ISSN 2321-0613, (2014) pp. 147-152
- [21] Sourav Das, Ameenur Rehman Siddiqui, Vishvendra Bartaria, "Evaluation of aluminium alloy brake drum for automobile application", vol. 2, issue 11, ISSN 2277-8616, (2013) pp. 96-102